

# Numerical simulation of the lateral load test on piles through a parametric analysis

Tatyanne P. dos Santos<sup>1</sup>, Aline da S. R. Barboza<sup>2</sup>

<sup>1</sup>*Dept. of Civil Engineering, University Center CESMAC  
R. da Harmônia, 57081-350, Maceió - Alagoas, Brazil  
[eng.pacifico@hotmail.com](mailto:eng.pacifico@hotmail.com)*

<sup>2</sup>*Laboratory of Scientific Computing and Visualization, Center of Technology, Federal University of Alagoas  
Av. Lourival Melo Mota, 57072-900, Maceió – Alagoas, Brazil  
[aline@lccv.ufal.br](mailto:aline@lccv.ufal.br)*

**Abstract.** Pile foundations are subjected to a significant number of lateral forces in addition to vertical forces. Models used to simulate soil-pile interaction under lateral loads include the Beam on Winkler Foundation (BWF) and the Nonlinear Beam on Winkler Foundation (BNWF), known as  $p$ - $y$  curves. This paper aims to investigate the impact of pile geometric properties, soil type, and the model used for simulating soil-pile interaction on the structural performance of a pile embedded in soil subjected to transverse loading. The study considers variations in three pile diameters (60 cm, 80 cm, and 100 cm), three pile lengths (5,5 m, 10,5 m, and 15,5 m), and two soil types (soft clay and stiff clay). The effects of pile diameter ( $D$ ), pile length ( $L$ ), slenderness ratio ( $L/D$ ), and soil consistency on the lateral response of the pile are examined. The results presented show that, depending on the soil type, modelling the soil with linear horizontal springs produces acceptable results, making the use of the nonlinear model unnecessary.

**Keywords:** soil-pile interaction,  $p$ - $y$  curves, Winkler.

## 1 Introduction

Pile foundations are used to transfer structural loads to the soil when the structure is supported on a layer of soil with low bearing capacity. For an axially loaded pile, the load is transferred to the soil through lateral friction at the soil-pile interface and the end bearing resistance provided by the soil. Pile foundations are subjected to significant lateral forces in addition to vertical forces. According to authors Kavitha, Beena, and Narayanan [1], the influence of vertical load on the lateral response of the pile is not as significant as the simultaneous action of both vertical and lateral loads. However, current design practices consider the influence of these two loads independently, which can lead to results that deviate from reality.

The lateral resistance of pile foundations depends on boundary conditions, stiffness, and strength of the pile, as well as the type of soil, soil stiffness, and soil strength. Studies have observed that the lateral resistances of both soil and pile are dominated by the characteristics of the soils near the applied lateral load, typically close to the ground surface. Soils below a certain depth do not significantly contribute to the pile's lateral resistance and stiffness due to the lateral deformation profile. This differs from piles subjected to axial loading, where soils along the entire effective length of the piles contribute to the axial resistance and stiffness of the pile (JIA [2]).

According to Velloso and Lopes [3], there are several models that analyse the support condition and provide horizontal displacements and internal forces for piles subjected to horizontal forces. In these models, the soil can be represented in two ways:

- (a) through an extension of the Winkler hypothesis, with linear and independent horizontal springs; and

(b) as a continuous medium, typically elastic.

The lateral resistance of a pile can also be modelled as a series of uncoupled horizontal springs, known as Winkler springs, as shown in Figure 1 (with springs representing lateral resistance p-y, axial resistance t-z, and bearing capacity q-z). Each Winkler spring is characterized by a load-displacement curve to simulate the mobilization of the surrounding soil resistance as the pile displaces. This load-displacement curve is commonly referred to as the p-y curve.

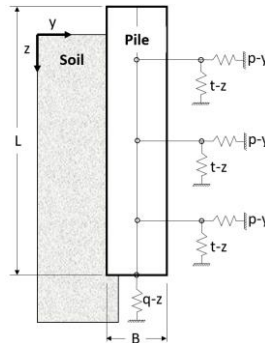


Figure 1. Modelling soil-pile interaction

The method of modelling non-linear soil springs using p-y curves, generally known as the p-y curve method, was developed by Reese, Cox, and Koop [4] and Reese, Cox, and Koop [5]. Semi-empirical methods are typically used to estimate p-y curves. There is a global trend towards using p-y curves for designing laterally loaded piles, which describe the non-linear relationship between soil resistance acting against the pile shaft ( $p$ ) and the lateral displacement of the pile ( $y$ ) (ARAÚJO [6]). In this context, this paper aims to conduct a parametric study to define the influence of pile diameter ( $D$ ), pile length ( $L$ ), slenderness ratio ( $L/D$ ), and soil type (soft clay and stiff clay) on the lateral response of the pile in terms of internal forces and lateral displacement.

## 2 Modelling Soil-Pile Interaction

Bapir et al. [7] conducted a state-of-the-art review describing the techniques commonly used for analysing buildings considering soil-structure interaction. The authors mention that soil mass modelling can be performed using both linear and non-linear models. Among the linear models presented is the Beam on Winkler Foundation (BWF). Among the non-linear models presented is the Beam on Non-Linear Winkler Foundation (BNWF). These highlighted models are considered simplified methods for analysing soil-pile interaction and, as such, can be easily applied in structural design practice.

### 2.1 Beam on Winkler foundation (BWF)

In this paper, the Beam on Winkler Foundation (BWF) was represented using the expression determined by Vesic [8], which calculates the horizontal subgrade reaction modulus through Equation 1. In this model, the case of a sufficiently long pile with diameter or side  $B$  and flexural stiffness  $EI$  is analyzed in a homogeneous and isotropic soil defined by an elasticity modulus  $E_s$  and a Poisson's ratio  $\nu_s$ .

$$K = 0,65 \cdot \sqrt[12]{\frac{E_s \cdot B^4}{EI}} \cdot \frac{E_s}{(1-\nu_s^2)} \quad (1)$$

According to Cintra [9], Equation 1 was originally derived and experimentally verified for beams with elastic support. However, this equation is also valid for interpreting the results of lateral load tests on piles in cases where the modulus of elasticity of the soil ( $E_s$ ) can be assumed constant.

### 2.2 Beam on non-linear Winkler foundation (BNWF)

A numerical simulation for the Beam on Non-Linear Winkler Foundation (BNWF) was performed in ABAQUS®. The numerical model consists of a circular concrete pile embedded in the surrounding soil and at the soil-pile interface. Only half of the model was simulated due to symmetry along the sectional plane, with appropriate constraints imposed on the symmetric face. The dimensions used were based on Faro [10], where in the  $x$ ,  $y$ , and  $z$  directions the dimensions were  $20D$ ,  $10D$ , and  $(L+3)$ , respectively, where  $D$  and  $L$  are the diameter and length of the pile. A geometry of the model is presented in Figure 2, with lateral and bottom boundaries fixed in the  $x$ ,  $y$ , and  $z$  directions. The boundary conditions for the numerical simulations included full constraint (fixed) at the bottom surface, freedom of movement in the  $z$  direction on the lateral surfaces, freedom of movement in the  $z$  direction on the front surface of the symmetry plane, and freedom of movement in the  $x$  and  $z$  directions, as well as rotation around the  $y$ -axis for the symmetry plane.

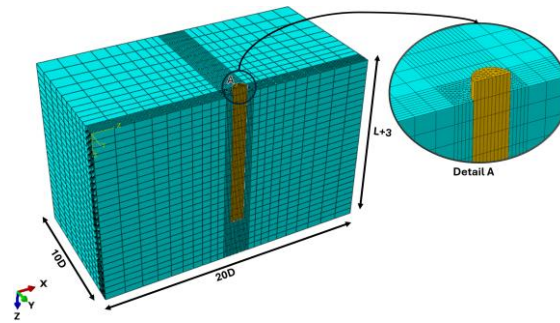


Figure 2. Three-dimensional numerical model used to simulate lateral load test on piles

Three diameters (60 cm, 80 cm, and 100 cm) and three lengths (5 m, 10 m, and 15 m) are considered for the pile, along with two types of soil (stiff clay and soft clay). It is important to note that all models incorporate an additional 0,5 meters in the pile length ( $L$ ) above the ground level to establish an appropriate dimension for the load application. The geometric characteristics of the model are presented in Table 1.

Table 1. Geometric characteristics of the numerical models

Models		$D$ (cm)	$L$ (m)	$L/D$
MD60L5AR	MD60L5AM	60	5,5	9,17
MD60L10AR	MD60L10AM	60	10,5	17,5
MD60L15AR	MD60L15AM	60	15,5	25,8
MD80L5AR	MD80L5AM	80	5,5	6,88
MD80L10AR	MD80L10AM	80	10,5	13,1
MD80L15AR	MD80L15AM	80	15,5	19,4
MD100L5AR	MD100L5AM	100	5,5	5,5
MD100L10AR	MD100L10AM	100	10,5	10,5
MD100L15AR	MD100L15AM	100	15,5	15,5

The nomenclature adopted for the models reflects the diameter ( $D$ ), pile length ( $L$ ), and the corresponding soil type. The abbreviations AR and AM are used to indicate the soil types: stiff clay and soft clay, respectively. For the materials used in the numerical models, a linear elastic behaviour is defined for the pile, while an elastoplastic perfectly plastic model with the Mohr-Coulomb failure criterion is adopted for the soils. The properties of the materials used are presented in Table 2. The soil parameters used in this study were derived through empirical correlations presented in Velloso and Lopes [3], using the Standard Penetration Test (SPT) as a reference. This method of obtaining soil strength is widely used in Brazil and, for this reason, was employed in this study.

Table 2. Material properties

Parameters	Concrete	
	Specific weight, $\gamma$ (kN/m <sup>3</sup> )	24
Poisson's ratio, $\nu$	0,15	
Elastic modulus, $E_c$ (MPa)	24150	
Parameters	Soil	
	Stiff clay	Soft clay
Standard Penetration Test index, $N_{spt}$	15	5
Specific weight, $\gamma'$ (kN/m <sup>3</sup> )	19	15
Poisson's ratio, $\nu_s$	0,21	0,23
Elastic modulus, $E_s$ (MPa)	15,75	5,25
Coefficient of earth pressure at rest, $K_0$	0,5	0,5
Cohesion, $c$ (kPa)	150	50
Internal friction angle, $\phi$ (degrees)	0	0
Dilation Angle, $\psi$ (degrees)	0	0

The numerical analyses were conducted by applying controlled deformations to the structure, providing greater precision and control when the resistance of the system reaches its limit. This procedure facilitates the convergence of the model. The horizontal load applied to the pile follows geotechnical engineering practice, as described by Faro [10]. It involves imposing a displacement at the top of the pile equivalent to 3% of its diameter, a value close to the total failure of the system.

The generation of  $p$ - $y$  curves in ABAQUS® is performed after processing the model, utilizing the principal stress (S11) and displacements in the same direction (U1), both in the  $x$ -direction. To analyse points of higher stresses,  $p$ - $y$  curves are generated for depths ( $z$ ) of 0,5 m (1), 1,0 m (2), 1,5 m (3), 2,0 m (4), and 2,5 m (5). Soil reactions ( $p$ , in force/length) at the mentioned depths are obtained by multiplying the stress  $S11$  at the analysed point by the diameter ( $D$ ) of the pile. This process allows the generation of the  $p$ - $y$  curve, relating soil reaction ( $p$ ) to horizontal displacement ( $y$ ) at each analysed point.

To obtain the horizontal reaction module ( $K$ ) for nonlinear springs, firstly, the  $p$ - $y$  modulus ( $E_{py}$ , in force/length<sup>2</sup>) is calculated by dividing the soil reaction ( $p$ ) by the horizontal displacement ( $y$ ) at the analysed point. Next, the horizontal soil reaction coefficient ( $kh$ ) is calculated by dividing the  $p$ - $y$  modulus ( $E_{py}$ ) by the pile diameter ( $D$ , in length units). Finally, the horizontal reaction module ( $K$ ) is obtained by multiplying the horizontal soil reaction coefficient ( $kh$ ) by the influence area, in this work  $D \times 0,5$  m (points were considered every 0,5 m).

### 3 Results and Discussions

#### 3.1 Parametric analysis of the effect of pile diameter (D)

In this study, the effect of diameter (60 cm, 80 cm, and 100 cm) on the lateral response of a pile with  $L = 10$  m embedded in cohesive soils (stiff and soft clays) is analysed. Figure 3 presents the results of internal forces and horizontal displacement for this initial analysis.

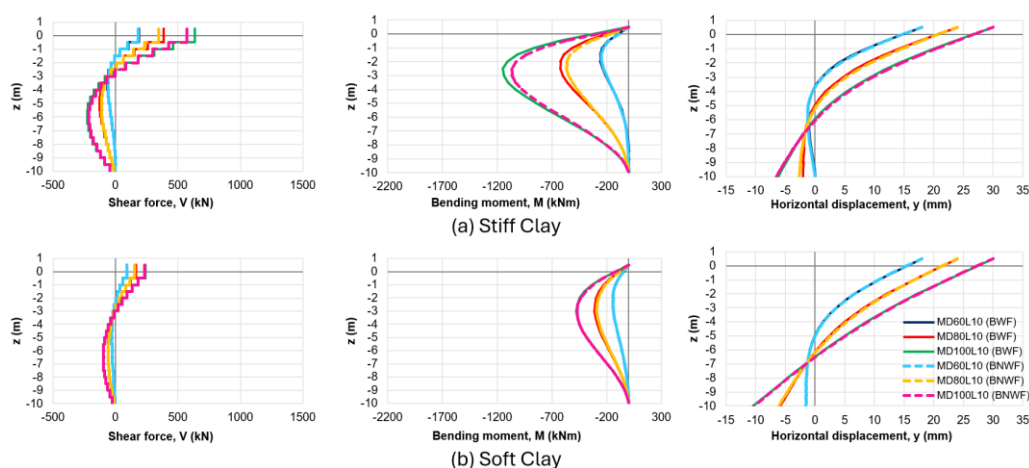


Figure 3. Effect of pile diameter on lateral response to internal forces and horizontal displacement

The results cited below will always be presented in ascending order of pile diameter, that is, 60 cm, 80 cm, and 100 cm. It is noteworthy that the results for BWF and BNWF are similar for both clays. In the analysis of the results for the pile in stiff clay, the difference between the maximum shear force values is 3%, 11%, and 10%. For the pile in soft clay, the difference between the maximum shear force values is 0%, 8%, and 4%.

When evaluating the maximum bending moment values, it is observed that for the pile in stiff clay, the maximum values occur at the pile embedment depths of 1,5 m, 2,5 m, and 2,5 m. These values are 260,01 kNm, 624,98 kNm, and 1146,53 kNm for the BWF model, and 248,82 kNm, 567,31 kNm, and 1067,21 kNm for the BNWF model.

For the pile in soft clay, the maximum bending moments occur at the pile embedment depths of 2,5 m, 3,0 m, and 3,0 m. The maximum values are 146,12 kNm, 309,38 kNm, and 476,53 kNm for the BWF model, and 145,24 kNm, 291,11 kNm, and 472,72 kNm for the BNWF model.

Analysing the BWF and BNWF models, the differences between the maximum bending moments for the piles in stiff clay are 4%, 9%, and 7%. For the pile in soft clay, the differences are 1%, 6%, and 1%.

In the analysis of lateral displacement, due to the characteristic of the test applying load or displacement at the top of the pile, the greatest displacements occur near this point of application and decrease with depth. Thus, the depth of the point of inflection of the horizontal displacements is evaluated according to the variation of the pile diameter.

For the pile in stiff clay, the points of inflection occur at depths of 5,0 m and 7,5 m for diameters of 60 cm and 80 cm. The pile with a diameter of 100 cm, due to its rigidity, has a less pronounced curvature, without an inflection point.

Finally, for the pile in soft clay, only the 60 cm diameter shows an inflection point at a depth of 6,0 m. The other diameters behave similarly to a rigid body within the soil, not developing a pronounced curvature.

### 3.2 Parametric analysis of the effect of pile length (L)

In this study, the effect of pile embedment length (5 m, 10 m, and 15 m) on the lateral response of a pile with diameter  $D = 80$  cm in cohesive soils is analysed. The subsequent results will be presented in ascending order of pile embedment length.

Based on the results presented in Figure 4, it is observed that the maximum shear forces occur at the point of displacement application, i.e., at the pile head. For the pile embedded in stiff clay, the maximum shear forces are 264,48 kN, 386,86 kN, and 388,63 kN, with the BWF model. With the BNWF model, the maximum values are 232,44 kN, 343,77 kN, and 346,45 kN. The differences between the BWF and BNWF models are 12%, 11%, and 11%, respectively.

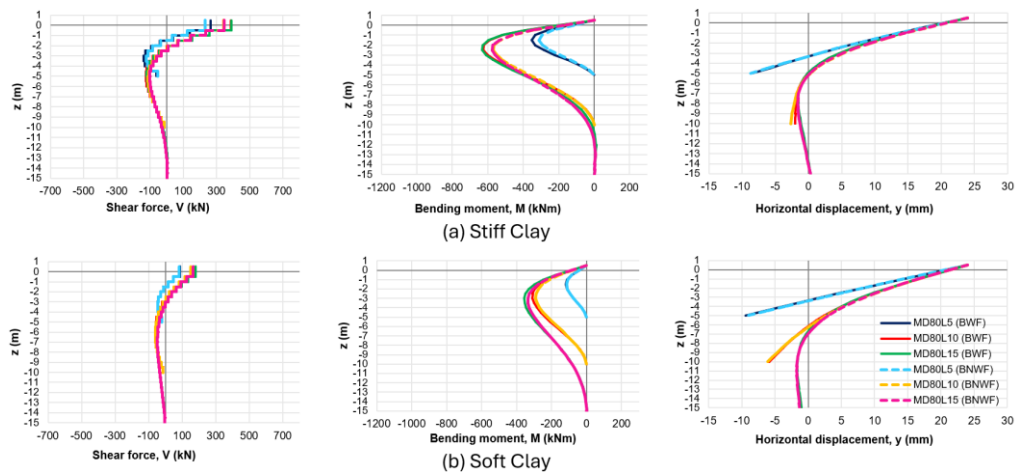


Figure 4. Effect of pile length on lateral response to internal forces and horizontal displacement

For the pile embedded in soft clay, the maximum shear forces are 87,01 kN, 166,49 kN, and 179,16 kN with the BWF model. With the BNWF model, the maximum values are 83,60 kN, 152,72 kN, and 165,09 kN. The differences between the BWF and BNWF models are 4%, 8%, and 8%, respectively. For all analysed models, the BWF resulted in higher shear forces compared to the BNWF.

When analysing the maximum bending moment values, it is observed that for the pile in stiff clay, the maximum moments occur at embedment depths of 1,5 m, 2,5 m, and 2,5 m. For the BWF model, the maximum bending moments are -352,12 kNm, -624,98 kNm, and -631,69 kNm. For the BNWF model, the maximum bending moments are -311,12 kNm, -567,31 kNm, and -575,88 kNm. The differences between the BWF and BNWF models are 12%, 9%, and 9%, respectively.

For the pile in soft clay, the maximum moments occur at embedment depths of 1,5 m, 3,0 m, and 3,0 m. For the BWF model, the maximum bending moments are -117,40 kNm, -309,38 kNm, and -355,87 kNm. For the BNWF model, the maximum bending moments are -114,84 kNm, -291,11 kNm, and -335,78 kNm. The differences between the BWF and BNWF models are 2%, 6%, and 6%, respectively. It is worth noting that for all analysed cases, the BNWF model yielded lower values than the BWF model.

In the analysis of horizontal displacements, it is observed that short piles, with a length of 5,0 m, exhibit rigid body behaviour. As the pile length increases, flexibility increases, leading to a tendency of convergence in results between the BWF and BNWF models. It is notable that longer piles develop greater curvature, with an inflection point occurring around 50% of the pile embedment length.

### 3.3 Parametric analysis of the slenderness ratio effect (L/D)

This study analyzes the effect of slenderness ratio ('5,5', '6,88', '15,5', and '19,38') on the lateral response of piles in cohesive and non-cohesive soils. These ratios were chosen to investigate the behavior of short, intermediate, and slender piles. It is important to note that the slenderness ratios '5,5', '6,88', '15,5', and '19,38' correspond to the models MD100L5, MD80L5, MD100L15, and MD80L15, respectively. The results presented below will be consistently shown in ascending order of slenderness ratio.

The results shown in Figure 5 indicate that the highest shear force occurs for the L/D ratio of 15,5 for both

soil types studied. In the analysis of the sturdier piles, with L/D ratios of '5,5' and '6,88', the highest shear force occurs at L/D = 5.5. Thus, it can be concluded that as slenderness increases, forces increase up to a certain point and then begin to decrease. When analysing the soil simulation models (BWF and BNWF), similar results are observed for piles embedded in stiff and soft clays.

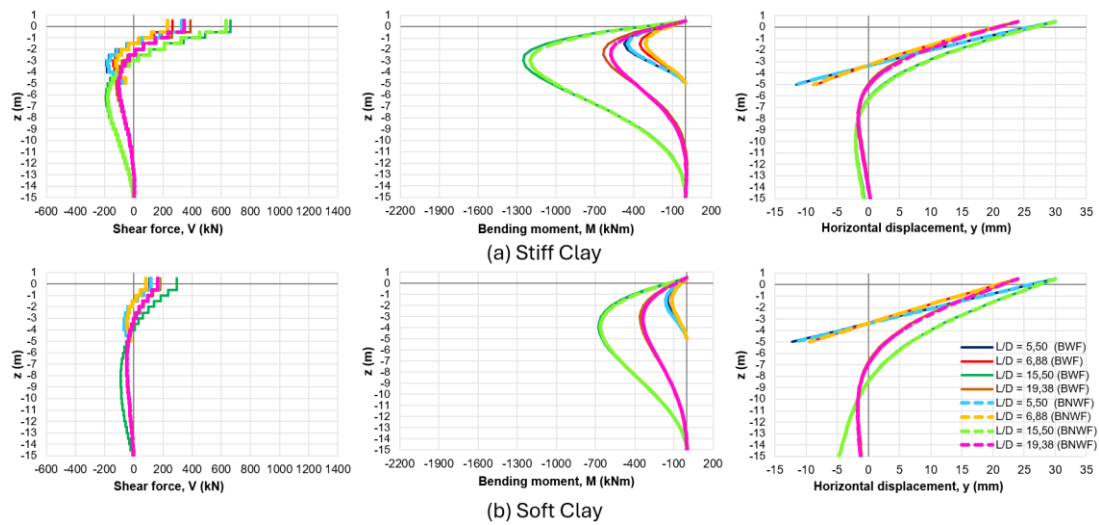


Figure 5. Effect of pile slenderness ratio on lateral response to internal forces and horizontal displacement

In the analysis of maximum shear forces, it is observed that for the pile embedded in stiff clay, the maximum values for the BWF model are 350,50 kN, 264,48 kN, 662,67 kN, and 388,63 kN. For the BNWF model, the maximum shear forces are 327,52 kN, 232,44 kN, 633,16 kN, and 346,45 kN. When analysing the differences between the BWF and BNWF models, percentages of 7%, 12%, 4%, and 11% are observed, respectively. In all cases, the BWF generated higher shear forces compared to the BNWF.

For the pile embedded in soft clay, the maximum shear forces for the BWF model are 110,88 kN, 87,01 kN, 293,56 kN, and 179,16 kN. For the BNWF model, the maximum shear forces are 115,46 kN, 83,60 kN, 166,53 kN, and 165,09 kN. Analysing the differences between the BWF and BNWF models shows percentages of 4%, 4%, 43%, and 8%, respectively. In the analysed models, the BWF yielded higher values than the BNWF, except for the slenderness ratio of '5,5'. It is important to note that for L/D = 15,5, the difference between the models is significant, which is not the case for the other slenderness ratios analysed.

Regarding the behaviour of the pile under bending moment, it is observed that for the pile embedded in stiff clay, the maximum values for the BWF model are -471,99 kNm, -352,12 kNm, -1253,42 kNm, and -631,69 kNm. For the BNWF model, the maximum bending moments are -446,36 kNm, -311,12 kNm, -1197,21 kNm, and -575,88 kNm. Analysing the differences between the BWF and BNWF models shows percentages of 5%, 12%, 4%, and 9%, respectively. In all cases, the BWF generated higher bending moments compared to the BNWF.

Lastly, in the analysis of lateral displacement, short piles behave as rigid bodies, without developing curvature. Longer piles develop curvature, with the inflection point occurring between 32% and 42% of the embedment length in stiff clay, and between 45% and 55% of the pile length in soft clay.

### 3.4 Parametric analysis of the effect of clay consistency

In this study, an analysis of the effect of clay consistency (soft or stiff) on the lateral response of a pile with a diameter  $D = 80$  cm and an embedded length  $L = 10$  m is performed.

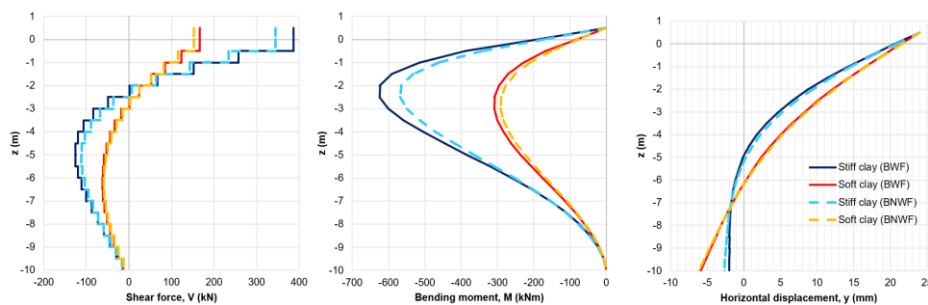


Figure 6. Effect of soil consistency on the pile response to internal forces and horizontal displacement

The results presented in Figure 6 show that the BWF model results in higher internal forces compared to the BNWF. The difference between the models is more evident in the analysis of maximum forces; for stiff clay, the difference is around 13% for shear force and 10% for bending moment, while for soft clay, it differs by 9% and 6%, respectively. For horizontal displacements, the BNWF model causes greater displacements compared to the BWF, with a divergence of 34% and 4% at the pile base in stiff and soft clay, respectively. Thus, it is possible to observe the influence of clay consistency on the pile behaviour from the horizontal displacement results: the pile in soft clay behaves similarly to a rigid body, unlike the pile in stiff clay, which developed a more pronounced curvature.

## 4 Conclusions

Through the conducted parametric study, it is possible to assess the impact of pile geometric properties, soil type, and the simulation model used in the soil-pile interaction on the structural behaviour of a pile subjected to horizontal displacement, considering internal forces and horizontal displacement. The results of the parametric study are presented in the following sections:

- (a) Effect of pile diameter (D): increasing this parameter results in higher internal forces along the shaft of the pile and smaller horizontal displacements.
- (b) Effect of pile length (L): shear forces decrease with increasing pile length. Longer piles exhibit higher bending moments and horizontal displacements along the shaft. There is a tendency towards rigid body behaviour for shorter piles.
- (c) Effect of slenderness ratio (L/D) of the pile: slender piles, when embedded in clay, experience higher shear forces and bending moments along the shaft. However, when embedded in sand, there is a tendency for internal forces to decrease. Short piles behave as rigid bodies, while long or slender piles may experience buckling.
- (d) Effect of clay consistency: piles in more flexible soils exhibit rigid body behaviour, while piles in stiffer soils are subjected to greater internal forces and show a more pronounced curvature in displacement.

The presented results demonstrate that the behaviour of pile foundations, considering soil-pile interaction, depends on various factors and should be rigorously evaluated by structural designers. Depending on the soil type, modelling the soil with linear horizontal springs yields acceptable results, obviating the need for nonlinear models.

**Acknowledgements.** The authors acknowledge the Laboratory of Scientific Computing and Visualization (LCCV), from Technology Center (CTEC) at Federal University of Alagoas (UFAL) for the support provided in this research. The first author acknowledges the support from the Research Foundation of the State of Alagoas (FAPEAL) to develop this work.

**Authorship statement.** The authors hereby confirm that they are the sole liable persons responsible for the authorship of this work, and that all material that has been herein included as part of the present paper is either the property (and authorship) of the authors, or has the permission of the owners to be included here.

## References

- [1] KAVITHA, P. E.; BEENA, K. S.; NARAYANAN, K. P. A review on soil–structure interaction analysis of laterally loaded piles. *Innovative Infrastructure Solutions*, v. 1, n. 1, 1 dez. 2016.
- [2] JIA, J. *Soil dynamics and foundation modeling*. New York: Springer, 2018.
- [3] VELLOSO, D. DE A.; LOPES, F. DE R. *Fundações: critérios de projeto, investigação do subsolo, fundações superficiais, fundações profundas*. São Paulo: Oficina de Textos, 2010. v. 1.
- [4] REESE, L. C.; COX, W. R.; KOOP, F. D. Analysis of laterally loaded piles in sand. *Offshore Technology Conference*, p. 473–484, 1974.
- [5] REESE, L. C.; COX, W. R.; KOOP, F. D. Field testing and analysis of laterally loaded piles in stiff clay. *Offshore Technology Conference*, p. 671–691, 1975.
- [6] ARAÚJO, A. G. D. DE. *Provas de carga estática com carregamento lateral em estacas escavadas hélice contínua e cravadas metálicas em areia*. Dissertação. Natal - RN: Universidade Federal do Rio Grande do Norte, 2013.
- [7] BAPIR, B. et al. Soil-structure interaction: a state-of-the-art review of modeling techniques and studies on seismic response of building structures. *Frontiers in Built Environment*, v. 9, 3 fev. 2023.
- [8] VESIC, A. B. Beams on elastic subgrade and the Winkler's hypothesis. *International Society for Soil Mechanics and Geotechnical Engineering*, p. 844–850, 1961.
- [9] CINTRA, J. C. A. *Carregamento lateral em estacas*. Escola de Engenharia de São Carlos, p. 1–88, 2002.
- [10] FARO, V. P. *Carregamento lateral em fundações profundas associadas a solos tratados: concepção, provas de carga e diretrizes de projeto*. Tese. Porto Alegre - RS: Universidade Federal do Rio Grande do Sul, 2014.